

MEMO No      CFD/TERMO-14-97

DATE: January 13, 1997

TITLE

IMPLEMENTATION OF THE COMPRESSIBILITY EFFECT IN TO DISSIPATION EQUATION OF A TWO-EQUATION TURBULENCE MODEL

AUTHOR(S)

Patrik Rautaheimo

ABSTRACT

In the  $k-\epsilon$  turbulence model the effect of compressibility is generally neglected and an incompressible version of the model is used. However, with high Mach numbers results can be improved by a compressible dissipation.

MAIN RESULT

Correction term owing to compressibility to the turbulent dissipation rate

PAGES

6

KEY WORDS

Dissipation, dilatation-dissipation, turbulent compressible flow

APPROVED BY

Timo Siikonen

January 13, 1997

## 1 Introduction

Compressibility effects to the dissipation of the turbulent kinetic energy can be taken account through an extra dissipation term. This extra term has an effect to lower the turbulent kinetic energy rates in compressible flow. It also has an effect in heat transfer rates after a shock wave. A more general discussion can be found in [1].

## 2 Methods

Chien [2]  $k - \epsilon$  turbulence model has been modified to take account dilatation-dissipation. According to Sarkar et al. [3] and Zeman [4],

$$\bar{\rho}\epsilon = \bar{\rho}(\epsilon_s + \epsilon_d) \quad (1)$$

where  $\epsilon_s$  is a solenoidal dissipation and  $\epsilon_d$  represents a compressible dissipation.

$$\epsilon_s = \bar{\nu} \overline{\omega_i'' \omega_i''} \quad \epsilon_d = \frac{4}{3} \bar{\nu} \overline{d''^2}. \quad (2)$$

Here  $d'' = u_{k,k}''$  denotes the fluctuating dilatation,  $\omega_i'' = \epsilon_{ijk} u_{k,j}''$  represent the fluctuating vorticity and  $\epsilon_{ijk}$  is the permutation tensor. The solenoidal dissipation can be represented by the ordinary dissipation equation

$$\frac{\partial \rho \epsilon_s}{\partial t} + \frac{\partial \rho u_i \epsilon_s}{\partial x_i} = \frac{\partial}{\partial x_i} \left[ (\mu + \mu_T / \sigma_\epsilon) \frac{\partial \epsilon_s}{\partial x_i} \right] + c_{\epsilon 1} f_1 \frac{\epsilon_s}{k} P - c_{\epsilon 2} f_2 \frac{\rho \epsilon_s^2}{k} + -2\mu(\epsilon_s / y_n^2) e^{-0.5y^+}. \quad (3)$$

Sarkar et al. [3] suggested for the compressible dissipation the following equation

$$\epsilon_d = Ma_t^2 \epsilon_s \quad (4)$$

where  $Ma_t = \sqrt{\overline{u_i'' u_i''}} / c$  is a turbulent Mach number and  $c$  is the speed of sound. Zeman model is more general [5]

$$\epsilon_d = \epsilon_s c_d \left\{ 1 - \exp \left[ - \left( \frac{M_{t^*} - M_{t_0}}{\sigma_M} \right)^2 \right] \right\} \quad (5)$$

where  $\epsilon_d = 0$  if  $M_{t^*} \leq M_{t_0}$ , with  $M_{t_0} = 0.2$ ,  $\sigma_M = 0.66$ ,  $c_d = 0.75$  and

$$M_{t^*} = \sqrt{\frac{2}{\gamma + 1}} M_t \quad (6)$$

Because of Sarkar's model simplicity we are going to use only it.

### 3 Results

#### Compressible Flat Plate

As a first test case, flow over a flat plate is simulated. The case is with a compressible turbulence in zero-pressure-gradient boundary layer. Measurements were performed by Fernholtz et al. [6]. A similar calculation has been made by Ladeinde et al. [5]. The Reynolds number per unit length,  $Re/m$  is  $6.5 \times 10^7/m$  and  $Ma_\infty = 2.87$ .

The length of the domain is  $0.6m$ , the height  $0.018m$  and the grid size is  $192 \times 64$ . The height of the first row of cells is  $2 \times 10^{-6}m$ . First three rows of the cells are kept constant and after that grid is clustered by ratio  $\Delta y_{j+1}/\Delta y_j = 1.119$ . Non-dimensional distance  $y^+$  is close to one at the first row. At the leading edge  $y^+$  is 3, and after 5 cells in axial direction, it is 1.

Inlet conditions are a uniform velocity distribution and pressure is extrapolated from the computational domain. Symmetry conditions are applied before the flat plate. At the flat plate, the velocities and kinetic energy of turbulence are set zero. The upper boundary parallel to the wall is assumed to be zero gradient. The second-order upwind scheme is used with Roe's flux splitting [7].

FINFLO INPUT file can be seen below

```

1      1      3      0      | IOLD  LEVEL  ITURB  NSCAL
/dionysos/tmp/rautahei/hilat/BOUNDARY_com.GRID
/dionysos/tmp/rautahei/boundary/Compressible/BOUND.BC
'ROE'  'YES'  'NO'  'NO'  'YES' | IFLX  RESTART STRESC FULLFC SOURC
'NO'   'YES'   0    0          | TIMEC  CONVC  PRESC  LUSGS
.5     .5     .00000001 64368. 1.0 | CFL-NUMBERS DROLIM TMAX DT1
10000  10000  1000    1          | ICMAX  KPRINT MPRINT IDRXX
0.0    0.000  00.0    0.000    | RMACH  ALPHA  BETA  ROTAT
0.0     0.72   0.90          | RE  PRANDTLIN LUVUT(PR;PRT)
1      'YES'          | ISTATE  STATEC
96.3   0.8478  0.      564.0    | FRSTEM  FRSDEN FRSPRE FRSVEL
0.0002 .1     5000.    1          | TURBLIM  RMULIM TURLIM IESPM
0.0003 .2     1.      2.      5. | TURBFRS  RMUFRS  CMGK CMGEPS CSIMPS
0      0      0      0          | JRDIF  JRDIS  JRPRE JRIMP
0.1     1.          | CC1  CC2
.6e-2   1.      1.          | AREF  CHLREF  GRILEN
0.      0.      0.      0.      -1. | XMOM  YMOM  ZMOM REFPRE DIFPRE
0.      0.      0.      0.          | GROUND GI  GJ  GK
4      3      0          | NUMBER OF BLOCKS  NOF INLETS/OUTLETS
192    64    01    +1 -3 -1  010 1 | IMAX JMAX KMAX INTER(IJK) LAMIN BLOCK 1
00     3     1     193 65  2  0 | IT  IL  IK  IDI1 IDI2 IDI3 MOV
2      1     192    3  64  1  01 | MGRID MIB MIT  MJB MJT  MKB MKT
0.      0     0          | OMEGA IROTVE  IGRID
2      64    01    +1 -1 -1  010 1 | IMAX JMAX KMAX INTER(IJK) LAMIN BLOCK 1
0      3     1     3  65  2  0 | IT  IL  IK  IDI1 IDI2 IDI3 MOV
1      1     2     3  64  1  01 | MGRID MIB MIT  MJB MJT  MKB MKT
0.      0     0          | OMEGA IROTVE  IGRID
192    2     01    +1 -1 -1  010 1 | IMAX JMAX KMAX INTER(IJK) LAMIN BLOCK 1
0      3     1     97  3  2  0 | IT  IL  IK  IDI1 IDI2 IDI3 MOV
1      1     96    1  2  1  01 | MGRID MIB MIT  MJB MJT  MKB MKT
0.      0     0          | OMEGA IROTVE  IGRID
2      64    01    +1 -1 -1  010 1 | IMAX JMAX KMAX INTER(IJK) LAMIN BLOCK 1
0      3     1     3  65  2  0 | IT  IL  IK  IDI1 IDI2 IDI3 MOV
1      1     2     3  64  1  01 | MGRID MIB MIT  MJB MJT  MKB MKT
0.      0     0          | OMEGA IROTVE  IGRID

```

Velocity profiles are compared at  $x = 0.5m$  with the experimental result

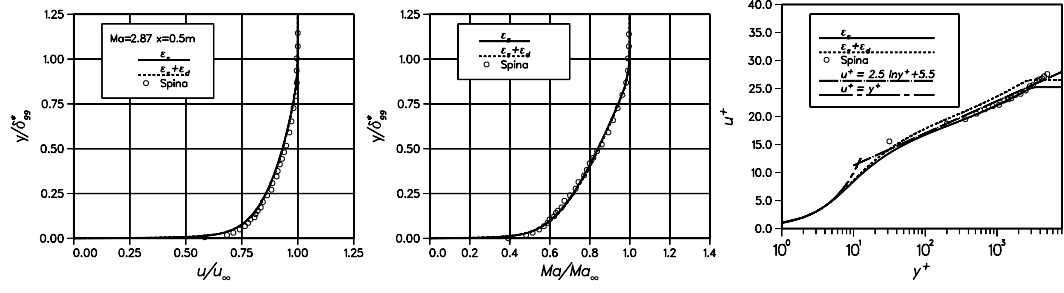


**Fig. 1:** Comparison of the velocity profiles with the measurements of Fernholtz et al. [6].

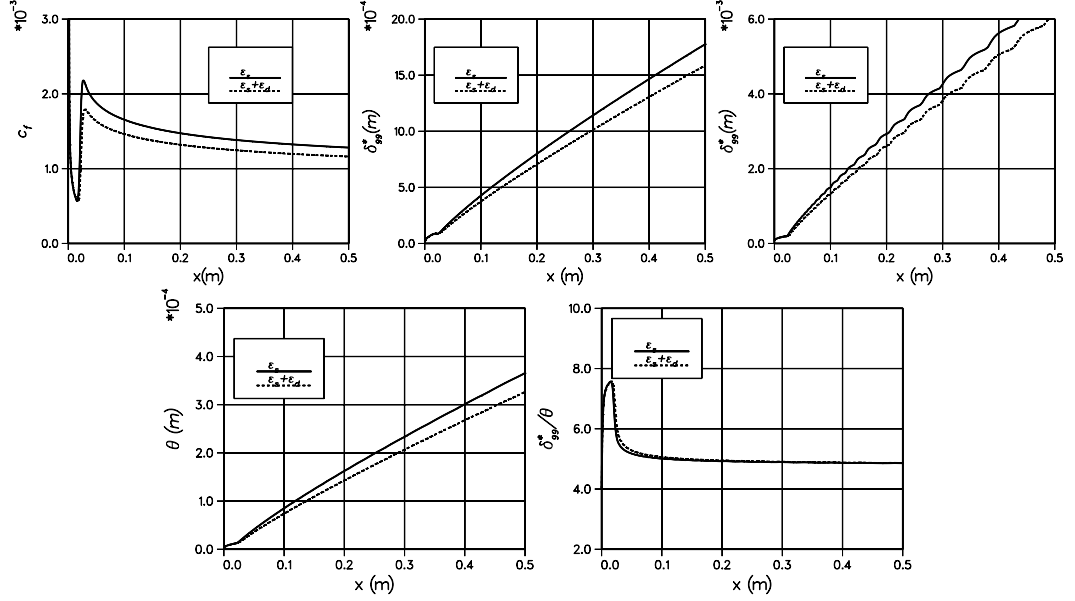


**Fig. 2:** Universal boundary layer parameters. From left to right: friction coefficient, boundary layer thickness, displacement thickness, momentum thickness and shape function.

in Fig. 1. Velocity profiles show good agreement with experiments. At the universal velocity profiles there is small variation between methods and experiments. Universal boundary layer parameters are shown in Fig. 2. Boundary layer parameters are in figure from left to right: friction coefficient  $c_f$ , boundary layer thickness at point where velocity is 99% of the free stream velocity  $\delta_{99}$ , displacement thickness  $\delta_{99}^*$ , momentum thickness  $\theta$  and shape function  $H = \delta_{99}^*/\theta$ . These variables are defined as

$$c_f = \tau_w / \left( \frac{1}{2} \rho U_e^2 \right) \quad (7)$$

$$\delta^* = \int_0^{\delta_{99}} \left( 1 - \frac{u(y)}{U_e} \right) dy \quad (8)$$

$$\theta = \int_0^{\delta_{99}} \frac{u(y)}{U_e} \left( 1 - \frac{u(y)}{U_e} \right) dy \quad (9)$$

where  $U_e$  velocity at the edge of the boundary layer. No experimental results were available. As it can be seen in Fig. 2 spreading rate and skin friction are smaller with compressible dissipation.

## NACA 0012

As a second test case, flow over a NACA 0012 airfoil is calculated at  $Ma = 0.799$ ,  $Re = 9 \times 10^6$  and  $\alpha = 2.26^\circ$ . A C-type grid with  $192 \times 64$  cells is used in the simulation. The outer boundary of the grid is 20 chord lengths from the airfoil, and the cell thicknesses on the surface varies from  $5 \times 10^{-6}$  at the leading edge to  $2 \times 10^{-5}$  at the trailing edge. Nondimensional distance  $y^+$  is from 2 to 5. Turbulence model is Chien [2]  $k-\epsilon$  with Sarkar's modification. No transition model is used and Chien's model simulates the transition by itself. In the simulation, transition take place just at the leading edge for both size. The case has been previously calculated by Siikonen [8]. Experimental results for the force coefficient and the pressure coefficient distribution is from Holst [9].

FINFLO INPUT file can be seen below

```

NACA 0012
1      1      3      0      | IOLD LEVEL ITURB NSCAL
/dionysos/tmp/rautahei/hilat/NACA2D.GRID
/dionysos/tmp/rautahei/naca2d/NACA.BC
'ROE'  'YES'  'NO'  'NO'  'NO'  | IFLX  RESTART STRESC FULLFC SOURC
'NO'   'YES'  0     0     0     | TIMEC  CONVC  PRESC  LUSGS
2.5    2.5    1.E-7 64368. 1.0   | CFL-NUMBERS DROLIM TMAX  DT1
5000   10000  1000   1     | ICMAX  KPRINT MPRINT IDRXX
0.799  2.26   00.0   0.0   | RMACH  ALPHA  BETA  ROTAT
9.E6   0.72   0.90   | RE     PRANDTLIN LUVUT(PR;PRT)
1      'YES'  | ISTATE STATEC
288.15 0.     0.     0.     | FRSTEM FRSDEN FRSPRE FRVEL
2.E-4  .1458 5000. 1     | RKLIM  MULIM  TURLIM IESPMA
0.001  1.0   0.10  0.2   5.   | TURBINI RMUINI CMGK  CMGEPS CSIMPS
0      0     0     0     | JRDIF  JRDIS  JRPRE  JRIMP
0.1    1.    | CC1    CC2
0.01   1.    1.    | AREF  CHLREF GRILEN
0.     0.    0.     0.   -1.   | XMOM  YMOM  ZMOM  REFPRE DIFPRE
0.     0.    0.     0.    | GROUND GI    GJ    GK
1      0     0     | NUMBER OF BLOCKS NOF INLETS/OUTLETS
192 64 01  +1 -3 -1 010 1 | IMAX  JMAX KMAX INTER(IJK) LAMIN BL 1
161 3 1 193 65 2 0 | IT  IL  IK  IDI1  IDI2  IDI3 MOV
3 1 192 2 64 1 01 | MGRID MIB MIT  MJB MJT MKB MKT
0. 0 0 | OMEGA IROTV E IGIRD

```

This case is calculated with and without Sarkar modification. Iteration history for both cases can be seen in Figure 3. Stability of both methods are similar. The force coefficients can be seen in Table 1. It can be seen that Sarkar's modification does just only slightly better than the ordinary dissipation equations. However, qualitatively the result is slightly better with Sarkar model. This can be seen in Figure 4. Sarkar's model simulates even a boundary layer separation, but separated region is far too short. This is a common phenomenon with  $k-\epsilon$  turbulence models. Also overprediction of the skin friction after a shock can be seen with both models.

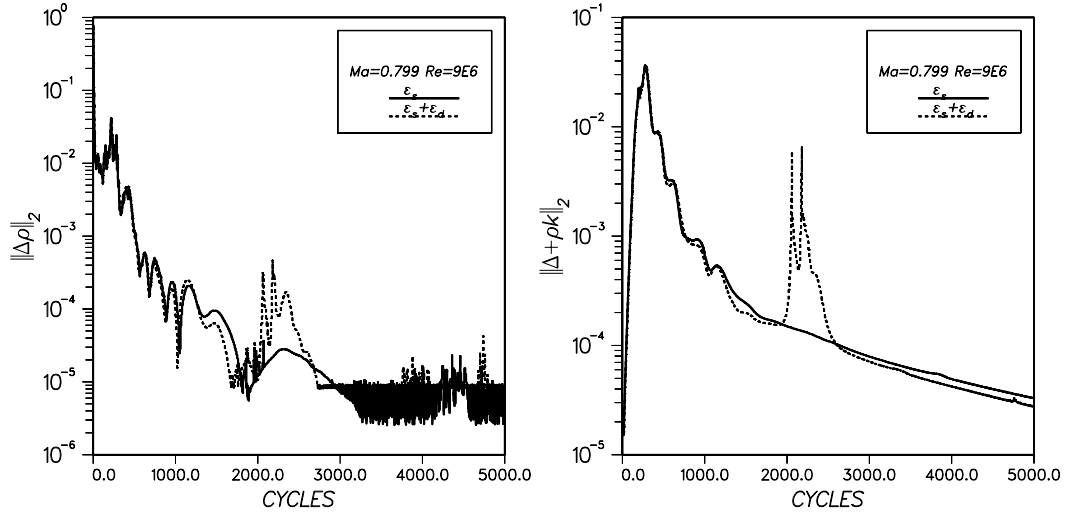


**Fig. 3:** Convergence history of the simulation.

**Table. 1:** Lift and drag coefficient.

	$c_l$	$c_d$	$c_l/c_d$
<b>Experimental</b>	0.390	0.0331	11.78
<b>Normal dissipation</b>	0.332	0.0391	8.49
<b>Sarkar model</b>	0.330	0.0382	8.64

## 4 Discussion

In these test cases the compressible dissipation did not have a big effect. It makes results a bit better. It reduces skin friction after a shock wave and also reduces the spreading rate of the boundary layer. The compressibility effects could be more visible with highly supersonic as hypersonic flows.

## References

- [1] Ladeinde, F., “Supersonic Flux-Split Procedure for Second Moments of Turbulence,” *AIAA Journal*, Vol. 33, July 1995, pp. 1185–1195.
- [2] Chien, K.-Y., “Predictions of Channel and Boundary-Layer Flows with a Low-Reynolds-Number Turbulence Model,” *AIAA Journal*, Vol. 20, Jan 1982, pp. 33–38.
- [3] Sarkar, S., Erlebacher, B., Hussaini, M., and Kreiss, H., “The Analysis and Modelling of Dilational Terms in Compressible Turbulence,” *Journal of Fluid Mechanics*, Vol. 227, 1991, pp. 473–493.

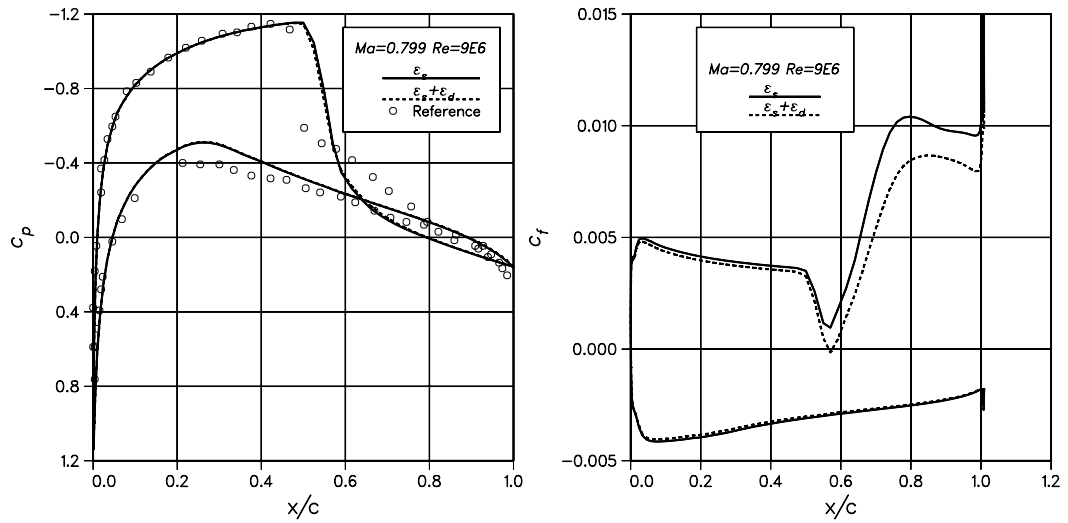


**Fig. 4:** Pressure and friction coefficient distributions.

- [4] Zeman, O., “Dilation dissipation: the Concept and Application in Modeling Compressible Mixing Layers,” *Phys. Fluids A*, Vol. 2, 1990, pp. 178–188.
- [5] Ladeinde, F. and Intile, J., “Calculation of Reynolds Stresses in Turbulent Supersonic Flows,” *International Journal for Numerical Methods in Fluids*, Vol. 21, 1995, pp. 49–74.
- [6] Fernholtz, H., Finley, P., Dussauge, J., and Smits, A., “A Survey of Measurements and Measuring Techniques in Rapidly Distorted Compressible Turbulent Boundary Layers,” AGARD 315, 1989.
- [7] Roe, P., “Approximate Riemann Solvers, Parameter Vectors, and Difference Schemes,” *Journal of Computational Physics*, Vol. 43, 1981, pp. 357–372.
- [8] Siikonen, T., “An Application of Roe’s Flux Difference Splitting for the  $k - \epsilon$  Turbulence Model,” Helsinki University of Technology, Laboratory of Aerodynamics, 1994. ISBN 951-22-2059-8.
- [9] Holst, T., “Viscous Transonic Airfoil Workshop Compendium of Results,” *Journal of Aircraft*, Vol. 25, Dec 1988, pp. 1073–1087.